1 **Targeting of NF-κB to Dendritic Spines is Required for Synaptic Signaling and**

2 **Spine Development**

3

4

5 **Authors:** Erica C. Dresselhaus[1], Matthew C.H. Boersma[2], and Mollie K. Meffert[1,2,#]

6

7 **Affiliations:**

8 [1]Department of Biological Chemistry

9 [2]Solomon H. Snyder Department of Neuroscience

10 [#]Corresponding author

11 The Johns Hopkins University School of Medicine, Baltimore, MD 21205, USA

12 Email: mkm@jhmi.edu

13

14 **Running Title: Dendritic Spine NF-κB Mediates Synaptic Signaling**
15 **Number of Pages: 33**
16 **Number of Figures:** 4
17 **Number of words: Abstract: 189, Significance: 120, Introduction: 571,**
18 **Discussion: 852**
19 **Conflict of interest:** The authors declare no competing financial interests.
20

26   sequence, and J.L. Pomerantz and members of the Meffert laboratory for discussion

27   and critical reading of the manuscript.

28

29   **ABSTRACT**

30   Long-term forms of brain plasticity share a requirement for changes in gene expression

31   induced by neuronal activity.   Mechanisms that determine how the distinct and

32   overlapping functions of multiple activity-responsive transcription factors, including

33   nuclear factor kappa B (NF-κB), give rise to stimulus-appropriate neuronal responses

34   remain unclear.   We report that the p65/RelA subunit of NF-κB confers subcellular

35   enrichment at neuronal dendritic spines and engineer a p65 mutant that lacks spine-

36   enrichment (ΔSEp65) but retains inherent transcriptional activity equivalent to wild-type

37   p65.   Wild-type p65 or ΔSEp65 both rescue NF-κB-dependent gene expression in p65-

38   deficient murine hippocampal neurons responding to diffuse (PMA/ionomycin)

39   stimulation.   In contrast, neurons lacking spine-enriched NF-κB are selectively impaired

40   in NF-κB-dependent gene expression induced by elevated excitatory synaptic

41   stimulation (bicuculline or glycine).   We used the setting of excitatory synaptic activity

42   during development that produces NF-κB-dependent growth of dendritic spines to test

43   physiological function of spine-enriched NF-κB in an activity-dependent response.

44   Expression of wild-type p65, but not ΔSEp65, is capable of rescuing spine density to

45   normal levels in p65-deficient pyramidal neurons.   Collectively, these data reveal that

46   spatial localization in dendritic spines contributes unique capacities to the NF-κB

47   transcription factor in synaptic activity-dependent responses.

48

SIGNIFICANCE STATEMENT

Extensive research has established a model in which the regulation of neuronal gene expression enables enduring forms of plasticity and learning. However, mechanisms imparting stimulus-specificity to gene regulation, insuring biologically appropriate responses, remain incompletely understood. NF-κB is a potent transcription factor with evolutionarily-conserved functions in learning and the growth of excitatory synaptic contacts. Neuronal NF-κB is localized in both synapse and somatic compartments, but whether the synaptic pool of NF-κB has discrete functions is unknown. This study reveals that NF-κB enriched in dendritic spines (the postsynaptic sites of excitatory contacts) is selectively required for NF-κB activation by synaptic stimulation and normal dendritic spine development. These results support spatial localization at synapses as a key variable mediating selective stimulus-response coupling.

INTRODUCTION

Elucidating the mechanisms that allow cells to make stimulus-appropriate responses remains one of the most compelling questions in the field of gene expression. While cell-type specific transcription is heavily influenced by promoter accessibility, factors conferring stimulus-specificity to transcription have remained more elusive. Post-mitotic neurons in the adult brain are capable of differential activity-dependent gene regulation in response to seemingly subtle differences in stimuli patterns, magnitude, and duration. Mechanisms that precisely regulate gene target specificity dictate changes in the complement of neuronal proteins and, ultimately, such

72 critical fates as whether neurons live or die, and whether synaptic connections are

73 appropriately strengthened, weakened, or eliminated during processes such as

74 information storage. Signaling cascades triggered downstream of neuronal activity by

75 neurotransmitters, growth factors, and cytokines can individually and cooperatively

76 induce multiple activity-responsive transcription factors, including CREB, Npas4, MEF2,

77 MeCP2 (Nonaka et al., 2014), and nuclear factor-kappaB (NF-κB) (Shrum and Meffert,

78 2008). How these discrete transcription factors contribute unique or overlapping

79 functions to disambiguate incoming signals and to orchestrate context appropriate

80 changes in gene expression remains incompletely understood.

81   NF-κB transcription factors exhibit evolutionarily-conserved requirements in a

82 wide variety of learning and memory paradigms (Freudenthal and Romano, 2000;

83 Meffert et al., 2003; Freudenthal et al., 2005; Kaltschmidt et al., 2006; O'Riordan et al.,

84 2006). NF-κB functions as a homo- or heterodimer of five possible mammalian

85 subunits: p65 (also termed RelA), RelB, c-Rel, p50, and p52. The p65:p50 heterodimer

86 is the most common NF-κB dimer in mammalian brain. Preformed NF-κB dimers are

87 held latent in the cytoplasm by the NF-κB inhibitor, IkappaB (IκB) until stimulus-induced

88 phosphorylation and degradation of IκB allows stable nuclear translocation of active NF-

89 κB. NF-κB is present in neuronal somatic and dendritic cytoplasm and has been

90 reported at synapses in both the *drosophila* neuromuscular junction (Heckscher et al.,

91 2007) and in the mammalian CNS (Kaltschmidt et al., 1993) where synaptic NF-κB can

92 be activated by excitatory stimulation (Meffert et al., 2003). Consistent with these

93 results, components of the NF-κB activation pathway are also localized at synapses

94 (Meffert et al., 2003). Previous work by our lab showed that NF-κB can be enriched in

95   the postsynaptic compartment of dendritic spines from hippocampal neurons (Boersma

96   et al., 2011), however, the potential for this localization to impart specific roles in

97   activity-dependent responses was unknown.

98   In this study, we demonstrate that the p65 subunit of NF-κB is required for

99   enrichment of the p65:p50 NF-κB dimer at dendritic spines and utilize a mutant p65

100 engineered to prevent spine-enrichment (p65ΔSE) to probe potential functions of NF-κB

101 subcellular localization near neuronal synapses. Our results show that neurons lacking

102 the spine-enriched pool of NF-κB are selectively deficient in NF-κB-dependent gene

103 expression by stimuli delivered through excitatory synapses, while remaining competent

104 to respond to stimulation that is not incoming through synapses. We assess a biological

105 role for the spine-enriched pool of NF-κB using a model of hippocampal developmental

106 synaptogenesis in which ongoing activation of NF-κB by elevated basal excitatory

107 neurotransmission (Meffert et al., 2003; Mihalas et al., 2013) is required for appropriate

108 dendritic spine formation (Boersma et al., 2011). In p65-deficient neurons, expression

109 of wild-type p65, but not p65 lacking spine-enrichment (p65ΔSE), can rescue normal

110 dendritic spine density in developing hippocampal neurons. Collectively, these findings

111 reveal that subcellular localization is a salient feature in producing stimulus-specificity

112 for activity-dependent gene expression and reveal a selective physiological function for

113 the spine-enriched pool of NF-κB transcription factor in response to excitatory

114 transmission and in dendritic spine development.

115

116 **MATERIALS and METHODS**

117 *Animals and Primary Cultures*

118   The care and use of mice met all guidelines of the local Institutional Animal Care and

119   Use Committee (The Johns Hopkins University School of Medicine).

120   Hippocampal neurons were dissociated from post-natal day 0 (P0) wild-type (ICR),

121   RelA$^{F/F}$, or GFPRelA$^{F/F}$ (De Lorenzi et al., 2009) male and female mouse pups and

122   prepared as described in (Boersma et al., 2011).   Cultures were transfected as

123   described in (Boersma et al., 2011).

124

125   *Imaging and quantification*

126   Confocal images of live murine hippocampal neurons were acquired on a Zeiss confocal

127   microscope (LSM5 Pascal), and analyzed as described (Boersma et al., 2011). Briefly,

128   fluorescence intensity in regions of interest (ROI) within dendritic spines and adjacent

129   dendritic shafts from Z-stacks containing the entire neurons or process of interest were

130   measured (ImageJ software) and analyzed using the following equations:

131   Normalized spine fluorescence (NSF) =

132   $(EGFP_{spine}/mCherry_{spine}) / (EGFP_{dendrite}/mCherry_{dendrite})$

133

134   Percentage change in fluorescence =

135   [NSF(p65tagged)-NSF(nontagged fluorescent protein)] / NSF(nontagged fluorescent

136   protein)

137

138   Spine enrichment for endogenous GFPp65 was analyzed using expressed mCherry to

139   mask the dendrite of interest (Imaris Bitplane software) and the spot function to place

140   and quantify fluorescence for mCherry and GFP in spine-head ROIs.

141

142 *Neuronal Stimulation*

143 DIV 20 - 21 hippocampal neuronal cultures from RelA$^{F/F}$ mice (+ OHT) expressing either

144 full length GFPp65 or GFPp65ΔSE were treated with synaptic or diffuse global stimuli at

145 37°C for 3.5 hours prior to harvest, as follows. For diffuse stimulation cultures were

146 treated with Ionomycin (2 µM, EMD, 407951) and phorbol 12-myristate 13-acetate

147 (PMA, 50 ng/ml, LC Labs, P-1680). For synaptic stimulation, neuronal cultures were

148 either treated with bicuculline or with glycine in a low-dose version of chemical LTP.

149 Bicuculline methobromide (30 µM, Tocris, 0109) was delivered for 30 seconds followed

150 by 1x stop solution (100x stock: 1 mM kynurenic acid, 1 M MgCl2, 0.3 M NaOH, 500

151 mM NaHEPES, pH 7.3). For low-dose glycine stimulation, neuronal cultures were

152 incubated with solution A (ACSF (130 mM NaCl, 3 mM KCl, 1.8 mM CaCl2 , 2 mM

153 MgCl2, 10 mM HEPES pH7.4, 10 mM D-Glucose), 1 µM Strychnine, 0.5 µM TTX (Tocris

154 Bioscience)) for 10 minutes at 37°C, followed by 10 minutes with solution B (ACSF-

155 0Mg + 150 µM Glycine, 1 µM Strychnine, 0.5 µM TTX) and then with solution A again for

156 3.5 hours at 37°C. Two distinct IKK (IκB kinase) inhibitors were used, where indicated.

157 The selective IKK inhibitor TPCA-1 (2-[(Aminocarbonyl)amino]-5-(4-fluorophenyl)-3-

158 thiophenecarboxamide, Tocris, 4 µM) or its vehicle, DMSO (dimethyl sulfoxide), or a

159 TAT peptide coupled membrane-permeant nemo binding domain (NBD) peptide (ENZO,

160 ALX-163-011) or control TAT peptide (ENZO, ALX-168-R050), both at 20 µM. IKK

161 inhibitors were pre-incubated with neuronal cultures for 30 minutes prior to stimulation.

162

163 *Expression constructs and lentiviral preparation*

164   Human p65, and p50 constructs were cloned by in-frame insertion using HindIII and

165   BamHI into the Clontech C1 vector at the C terminus of enhanced green fluorescent

166   protein (eGFP). p65 truncation mutants were created by PCR. Deletion mutants of p65

167   were created by two-step PCR.

168   PCR Primers:

169   p65Δ1-298: F-GTACGTAAGCTTCTGAGAAACGTAAAAGGACATATG,

170   R-GTACGTGGATCCTTAGGAGCTGATCTGACT

171   p65Δ305-406: F1-GTGCAAGCTTTAGACGAACTGTTCCCCCTCATCTTCCCG,

172   R1-CGTAGGATCCAAGGAGCTGATCTGACTCAGCAGGGCTGA,

173   F2-AAACGTAAAAGGACAGCCCCAGCCCCTGTCCCAGTC,

174   R2-GACAGGGGCTGGGGCTGTCCTTTTACGTTTCTCCTCAATCCGGTG

175   p65Δ335-442: F1-GTGCAAGCTTTAGACGAACTGTTCCCCCTCATCTTCCCG,

176   R1-CGTAGGATCCAAGGAGCTGATCTGACTCAGCAGGGCTGA,

177   F2-AAACGTAAAAGGACAGCCCCAGCCCCTGTCCCAGTC,

178   F2-ATTGCTGTGCCTTCCCAGCTGCAGTTTGATGATGAAGACCTGGGG,

179   R2-ATCAAACTGCAGCTGGGAAGGCACAGCAATGCGTCG

180

181   Lentivirus production from eBFP2-CreER^{T2} and eGFP2-CreER^{T2} were as described

182   (Boersma et al., 2011; Mihalas et al., 2013). Hippocampal cultures from RelA$^{f/f}$ mice

183   were infected with CreER^{T2} -expressing lentivirus at DIV 2 and treated with tamoxifen

184   (OHT; 400nM, Sigma-Aldrich H6278) to elicit recombination for 4 days prior to

185   experimentation.

186

187 *Reporter assays*

188 Luciferase reporter assays were performed as described (Mihalas et al., 2013) by co-

189 expressing firefly luciferase under the control of a promoter containing one or three NF-

190 κB consensus binding sites in HEK293T and neurons, respectively, together with

191 constitutively-expressed β-galactosidase (from pEF-Bos-LacZ), which was used to

192 normalize for transfection efficiency and extract recovery.

193

194 *Immunocytochemistry and immunoblotting*

195 Hippocampal neuronal cultures from GFPRelA$^{F/F}$ mice were fixed at DIV 16 as

196 described (Boersma et al., 2011) and subjected to immunohistochemistry with the

197 following primary antibodies: chicken anti-GFP (AVES, GFP-1020,1:1000), rabbit anti-

198 DsRed (Clontech, 632496, 1:500), and with secondary antibodies FITC anti-chicken

199 (GeneTex, GTX77185, 1:500) and Alexa Fluor 568 anti-rabbit (Invitrogen,

200 A11011,1:500) for 1 hour at room temp. in 10% BSA. Cells were mounted in 0.1M n-

201 propyl gallate in 50% glycerol.

202 For immunoblotting, equivalent total protein levels (by BCA protein assay) from lysates

203 were resolved by 12.5% SDS-PAGE gel electrophoresis followed by transfer to PVDF

204 membrane and probed using: anti-p65 (Santa Cruz Biotechnology, sc372, 1:5000),

205 anti-GFP (Neuromab, N86/8, 1:500 or Molecular Probes, A11122, 1:2000), anti-HSC70

206 (Santa Cruz Biotechnology, sc-7298, 1:10000).

207

208 *Electromobility shift assay*

209 EMSAs were carried out using nuclear or cytoplasmic extracts prepared from isolated

210 synaptosomes essentially as described (Meffert et al., 2003) and were reproduced 4

211 times. Extracts were incubated with a radiolabeled DNA oligonucleotide probe

212 containing the κB sequence (wild-type: GGGGACTTTCC, mutant: GTTGACTTTCC).

213

214 *Statistical analyses*

215 Graphs illustrate the arithmetic mean and error bars are SEM. For statistical analyses,

216 unless otherwise noted two-tailed, unequal-variance *t* tests were used with α = 0.05. For

217 ANOVA, one-way ANOVA with Bonferroni-Holm correction or Dunnetts correction was

218 used. For unequal sample sizes, a Kruskal-Wallis test followed by posthoc Dunn's

219 multiple comparison tests was performed where indicated.

220

221 **RESULTS**

222 **The p65 subunit of NF-κB is sufficient for localization to isolated synapses**

223 We previously demonstrated that the p65 subunit of NF-κB is present primarily

224 as a p65:p50 heterodimer in synapses isolated from murine hippocampi

225 (synaptosomes), and that genetic deletion of p65 led to the absence of NF-κB from

226 these synapses (Meffert et al., 2003). Multiple functional dimers of NF-κB exist in

227 mammalian neurons, including p65:p50, p50:p50, and p65:p65 in the murine

228 hippocampus. To investigate the subunit requirements for localization of NF-κB to

229 neuronal synapses, we initially evaluated the effect of loss of the p50 subunit on the

230 presence of NF-κB in isolated synapses. Biochemically isolated hippocampal synapses

231 (synaptosomes) from mice wild-type for p50 or lacking the p50 subunit of NF-κB were

232   subjected to electromobility shift assays (EMSA) with a radiolabeled DNA probe

233   containing the κB sequence and antibody supershifts used to identify discrete NF-κB

234   subunits. EMSA detects activated NF-κB dimers that are not IκB-bound and so are

235   able to bind and shift the mobility of the DNA probe. Deoxycholate (DOC), to force

236   dissociation of IκB, was included in some samples to reveal any occult (IκB bound) NF-

237   κB, so that we would not fail to identify present but inactive forms of NF-κB (Meffert et

238   al., 2003). We observed that isolated synapses from p50-deficient mice retained NF-κB

239   consisting of p65:p65 homodimers as shown by the supershifted band in the presence

240   of p65 antibody (Figure 1A; representative EMSA from 4 biological replicates). p65:p65

241   homodimers were present in increased abundance in the absence of the p50, in

242   comparison to synapses isolated from wild-type neurons which contained predominantly

243   p65:p50 heterodimers and small amounts of p65:p65 homodimers (Figure 1A). These

244   results were consistent with p50 (when present) as the known preferred subunit binding-

245   partner of p65, but demonstrated that, in the absence of p50, p65:p65 homodimers

246   could localize to synapses. Since NF-κB is not detected in synapses isolated from p65-

247   deficient neurons (Meffert et al., 2003), these results are collectively consistent with the

248   p65 subunit being necessary as well as sufficient for significant localization of NF-κB to

249   isolated hippocampal synapses.

250

251   **The p65 subunit of NF-κB, but not the p50 subunit, is enriched within dendritic**

252   **spines**

253   While biochemically isolated synapses can contain both pre-and post-synaptic

254   elements, our previous work suggested that NF-κB was enriched in dendritic spines, the

255   postsynaptic sites of excitatory synaptic contacts. Green fluorescent protein-tagged p65

256   (GFPp65) was enriched in spines of intact wild-type hippocampal neurons (Boersma et

257   al., 2011) in which the p65:p50 dimer of NF-κB predominates (Meffert et al., 2003). To

258   investigate whether p65 or p50 subunits were responsible for dendritic spine

259   enrichment, we first excluded the possibility of p50 heterodimerization with p65, by

260   assaying p50 spine-enrichment in neurons lacking p65.   Hippocampal neuronal

261   cultures from mice harboring a conditional loss of function allele for the RelA gene

262   (encoding p65 protein, RelA$^{F/F}$) were transduced with lentiviral inducible Cre

263   recombinase (CreER^{T2}) to generate p65-deficient cultures following administration of 4-

264   hydroxy-tamoxifen (OHT).   p65-deficient cultures co-expressing non-tagged mCherry

265   fluorescent protein (for visualization and quantification) with either GFP-tagged p50

266   (GFPp50), GFPp65, or GFP alone, were subjected to confocal imaging and analysis for

267   spine enrichment (calculation described in Materials and Methods). In the absence of

268   endogenous p65, no spine enrichment of GFPp50 was observed (0.9 ± 1.2%), while

269   GFPp65 retained its expected enrichment (39.7 ± 2.08%, p = 3.8 x 10^{-10}) relative to

270   GFP (Figure 1B). These results indicate that the p65 subunit of NF-κB is sufficient for

271   hippocampal spine enrichment, and that p65 likely mediates spine enrichment of the

272   predominant p65:p50 heterodimer.

273

274   **Characterization of spine parameters for p65 enrichment**

275   Variation in the morphological parameters of dendritic spines, including size and

276   head-to-neck ratio, have been shown to predict features such as spine stability and the

277   presence of functional synapses (Nimchinsky et al., 2002; Holtmaat and Svoboda,

278   2009). In multiple brain regions, including the hippocampus, larger spine head diameter

279   relative to neck diameter correlates with increased spine maturity and functional

280   synapses, in comparison to stubby spines or spines lacking a head (Peters and

281   Kaiserman-Abramof, 1970; Harris et al., 1992; Hering and Sheng, 2001; Tada and

282   Sheng, 2006). We next investigated the possibility of a relationship between spine

283   morphology and the extent of p65 enrichment in dendritic spines. Confocal Z-stacks of

284   dendritic spines from hippocampal neurons co-expressing GFPp65 and mCherry were

285   analyzed to calculate the ratio of dendritic spine head diameter to neck diameter (Figure

286   1C), as well as spine enrichment of GFPp65. Spines were considered any protrusion

287   between 0.2 μm to 3.0 μm with or without a head. For comparison and based on

288   published characterizations, spines were classified into 4 categories: spines in which

289   the head to neck ratio was ≤ 1, between 1 - 3, between 3 - 4, or > 4.   Spines in which

290   the head to neck diameter ratio was ≤ 1 (i.e. lacking a distinct head) did not exhibit

291   significant enrichment of GFPp65 at the spine terminus (GFPp65 spine enrichment of

292   7.99 ± 6.04%, p = 0.056 compared to GFP alone) (Figure 1D). In contrast, all three

293   spine categories with head to neck diameter ratio ≥ 1 had significantly more GFPp65

294   spine enrichment than spines with head to neck ratio ≤ 1 (p ≤ 0.003, ANOVA p = 0.005,

295   Dunn test for nonparametric data p ≤ 0.01). A trend was observed for greater GFPp65

296   enrichment with increasing spine head to neck ratio: head to neck ratio 1-3 (average

297   enrichment 33.57 ± 2.47%), head to neck ratio 3 - 4 (average enrichment 41.41 ±

298   6.31%), head to neck ratio > 4 (average enrichment 46.81 ± 9.34%) (Figure 1D), but this

299   did not reach significance (ANOVA, p = 0.159). These data indicated that GFPp65 was

300   more enriched in head-containing spines with a greater likelihood of mature synaptic

301 connections and suggested the possibility of a role for NF-κB at functional excitatory

302 synapses.

303

304 **p65 expressed from the endogenous locus is enriched in dendritic spines**

305 While expression of exogenous constructs was routinely titrated to the lowest

306 possible levels, we sought to further test the possibility of inappropriate p65 localization

307 due to overexpression artifact prior to further investigation. Anti-p65 antibodies

308 competent for immunoblotting have been identified, however, antibodies capable of

309 reliable brain immunostaining without staining in p65-deficient brain tissue were not

310 identified despite candidate screening. For this reason, we proceeded to assess

311 whether expression from the endogenous locus of p65 would similarly exhibit p65

312 enrichment in dendritic spines using a homozygous transgenic knock-in mouse line

313 expressing the fusion protein of GFP and p65 (GFPp65) from the genomic RelA locus

314 with GFP inserted immediately following the start codon (GFPRelA$^{f/f}$) (De Lorenzi et al.

315 2009). Notably, characterization of this line demonstrates GFPp65 expression to be

316 equal to endogenous p65 expression in wild-type mice, and to fully rescue endogenous

317 p65 function (p65 loss is embryonic lethal).

318 Hippocampal cultures from GFPRelA$^{f/f}$ mice were transfected with mCherry to

319 permit morphological isolation of individual neurons and enrichment quantification, and

320 subjected to immunostaining for GFP and mCherry (see Materials and Methods),

321 followed by confocal microscopy and 3-dimensional analysis of Z-stack projections

322 (Imaris). p65 expressed from the endogenous locus was enriched in hippocampal

323 dendritic spines by $33.5 \pm 6.9\%$ ($p = 1.36 \times 10^{-5}$) relative to non-tagged GFP (Figure 1E);

324   this enrichment was not significantly different from the dendritic spine enrichment of

325   transiently-transfected GFPp65 as shown in Figure 1B (p = 0.27). These results

326   supported the use of GFPp65 constructs expressed at low levels in subsequent

327   experiments to investigate the determinants of p65 enrichment.

328

329   **A p65 deletion mutant lacking dendritic spine-enrichment**

330   We next engineered a series of deletion and truncation constructs (Figure 2A)

331   aimed at identifying a mutant of the p65 subunit that would lack dendritic spine-

332   enrichment and allow us to examine potential physiological roles of a synaptic pool of

333   NF-κB. All NF-κB subunits share a highly homologous amino-terminal domain, known

334   as the Rel Homology Domain (RHD), which contains sequences responsible for DNA

335   binding, dimerization, IκB binding, and nuclear localization. p65 also contains a

336   carboxy-terminal trans-activation domain (TAD), which is a shared feature of several

337   NF-κB subunits (Napetschnig and Wu 2013). Amino-terminally GFP-tagged p65

338   truncations lacking either the carboxy-terminal TAD (p65ΔTAD) or the amino-terminal

339   RHD (p65Δ1-298) were co-expressed with non-tagged mCherry fluorescent protein in

340   hippocampal pyramidal neurons, subjected to confocal imaging, and found to retain

341   dendritic spine enrichment that did not significantly differ from wild-type GFPp65 (40.8 ±

342   4.9%, p = 0.813 and 40.29 ± 3.95% p = 0.980 respectively,) (Figure 2B and 2C). In

343   contrast, a p65 truncation consisting solely of the amino-terminal RHD including the

344   NLS (GFPp65Δ305-551), lacked enrichment in dendritic spines and was not significantly

345   different in enrichment compared to GFP (-4.2 ± 2.4%, p = 0.142). Collectively these

346   data, prompted us to focus on the region between the NLS and the TAD of p65, a

347   relatively uncharacterized region with little sequence conservation between NF-κB

348   subunits, which we suspected might be involved in dendritic spine enrichment.

349   Two constructs with overlapping deletions in p65 between the NLS and TAD

350   (p65Δ305-406 and p65Δ335-442) were engineered to refine the region required for

351   enrichment. Equivalent expression of these GFP-tagged constructs in hippocampal

352   pyramidal neurons co-expressing mCherry revealed that p65Δ335-442 retained

353   significant enrichment in comparison to GFP alone, while enrichment remained lower

354   than for full-length p65 (19.1 ± 3.5%, p = 4.67x10^{-5} and p = 0.002) (Figure 2B,C). In

355   contrast, p65Δ305-406 lacked significant spine enrichment (5.5 ± 2.2%, p = 0.102

356   compared to GFP alone), and we termed this mutant, GFPp65ΔSE. All truncation and

357   deletion p65 constructs were expressed at similar levels, as assessed by visualization

358   of the GFP-tag in confocal imaging (Figure 2C), and yielded protein products of the

359   expected molecular weights by immunoblotting of lysates from transfected 293T cells

360   (Figure 2D).

361   Due to the known participation of NF-κB in apoptotic pathways, we evaluated

362   GFPp65ΔSE expression for potential effects on neuronal cell health prior to proceeding

363   to other assays of physiological function. Dysregulation of NF-κB signaling in some

364   contexts can produce apoptosis which has been visualized as fragmented or pyknotic

365   nuclei or as cytoplasmic blebbing or beading (Baichwal and Baeuerle, 1997). We

366   assessed cytoplasmic integrity and nuclear morphology by confocal imaging of live

367   hippocampal neurons expressing either GFP, GFPp65 or GFPp65ΔSE for 24 hours,

368   together with mCherry fluorescent protein to fill the cytoplasm and Hoechst staining to

369   visualize nuclei. The experimenter was blinded to condition during all imaging and

370   analysis. Quantification showed no differences in cytoplasmic blebbing (GFP: 19.2%, n

371   = 9 cells; GFPp65: 0%, n = 8; GFPp65ΔSE: 12.5%, n = 8) or pyknotic nuclei (GFP:

372   11.1%, n = 9 cells; GFPp65: 12.5%, n = 8; and GFPp65ΔSE: 12.5%, n = 8) between

373   neurons expressing GFP, GFPp65, or GFPp65ΔSE (Figure 2E).   In contrast,

374   cytoplasmic blebbing and pyknotic, condensed and fragmented nuclei were readily

375   detected in 63.6% and 72.7%, respectively, of control neurons (n = 11) expressing GFP

376   and treated with the kinase inhibitor, staurosporine (50 nM, 12hr) to induce apoptosis

377   (Figure 2E). These results indicated that GFPp65ΔSE expression did not adversely

378   affect neuronal health as monitored by nuclear morphology and cytoplasmic

379   blebbing/beading. We proceeded to assess the transcriptional function of GFPp65ΔSE,

380   in comparison to wild-type p65.

381

Non-spine enriched p65 mutant retains basal transcriptional activity

383   We first examined whether the inherent transcriptional properties of wild-type p65

384   were altered in GFPp65ΔSE. While the region of p65 between the RHD and TAD,

385   containing the deletion in GFPp65ΔSE, has not been previously shown to contain

386   domains implicated in transcriptional regulation, we directly assessed the inherent

387   capacity of GFPp65ΔSE to induce NF-κB dependent transcription in comparison to wild-

388   type p65 (GFPp65) by dose titration in an NF-κB reporter assay. This reporter assay

389   effectively assesses multiple aspects of the NF-κB transcription factor, including

390   appropriate protein folding, stability, dimerization, DNA-binding, and transactivation

391   capacity.   The relative inherent activity of an NF-κB construct is evaluated by this

392   reporter assay in heterologous cells, without the need for cellular stimulation to mediate

393   IκB inhibitor degradation, through moderate overexpression of NF-κB subunits which

394   intentionally outstrips endogenous IκB to allow assessment of transcription activation.

395   HEK293T cells were co-transfected with NF-κB luciferase reporter and a constitutively

396   expressed β-galactosidase for normalization, in combination with either full length

397   GFPp65 or GFPp65ΔSE at increasing doses which were titrated for equivalent levels of

398   protein expression by immunoblot (Figure 3A, right).   Full length GFPp65 and

399   GFPp65ΔSE could each similarly activate NF-κB-dependent transcription from the

400   luciferase reporter across a range of expression levels in the dose titration (Figure 3A,

401   left). We conclude that deletion of amino acids 305-406 in p65ΔSE lacks measurable

402   impact on the inherent capability of p65 to induce NF-κB-dependent transcription.

403

404   **Non-spine enriched p65 mutant is not activated by a synaptic stimulus**

405   We next conducted experiments in hippocampal pyramidal neurons aimed at

406   addressing whether loss of spine enrichment might selectively alter NF-κB-dependent

407   transcription in response to stimuli originating at the excitatory glutamatergic synapses

408   which occur predominantly on dendritic spines, in comparison to stimuli with a diffuse

409   origin.   Following robust excitatory synaptic activation, suprathreshold ion fluxes or

410   second messenger signals can traverse from dendritic spines to dendritic and somatic

411   compartments (Nimchinsky et al., 2002). However, signals (including calcium

412   elevations) initiated by lower and physiological levels of synaptic activity, can be either

413   restricted to activated dendritic spines or near-neighbor spines (Nimchinsky et al., 2002;

414   Noguchi et al., 2005), or diminished prior to reaching the neuronal soma (Andersen et

415   al., 1980; Yuste et al., 2000). This prompted us to ask whether one role of a spine-

416   localized pool of NF-κB might be to preferentially regulate gene expression in response

417   to incoming stimuli in which signals are spatially restricted or of greater amplitude near

418   excitatory synapses on dendritic spines. To test this hypothesis we examined whether

419   modest excitatory synaptic stimulation could activate NF-κB lacking dendritic spine

420   enrichment (GFPp65ΔSE) as effectively as wild-type NF-κB (GFPp65) which is spine-

421   enriched. The participation of endogenous p65 was excluded by conducting NF-κB

422   reporter assays in p65-deficient hippocampal cultures prepared from RelA$^{f/f}$ mice.

423   Mature neuronal cultures (DIV20-21, when basal excitatory activity is low) were co-

424   transfected with NF-κB reporter and constitutively-expressed β–galactosidase, and low

425   levels of either full-length GFPp65 or GFPp65ΔSE. GFPp65ΔSE and GFPp65 were

426   expressed at similar levels as assessed by immunoblot (Figure 3B, inset) and

427   fluorescence confocal imaging. Neurons were then treated with either stimuli which

428   enhance endogenous excitatory synaptic transmission or with a diffuse stimulus not

429   originating at synapses. Synaptic stimulation was delivered using low-dose bicuculline

430   (30 μM for 30 seconds), a GABA$_A$ receptor inhibitor that enhances endogenous

431   glutamatergic excitatory transmission, or low-dose glycine (a chemical LTP protocol

432   stimulating NMDA receptors only at synapses receiving spontaneously released

433   glutamate)(Fortin et al., 2010; Araki et al., 2015). Calcium ionophore (ionomycin, 2 μM)

434   and phorbol ester (PMA, 50 ng/ml) were used to deliver diffuse generalized stimulation.

435   Both synaptic and diffuse stimuli have been previously characterized as activators of

436   endogenous NF-κB (Meffert et al., 2003). In the absence of stimulation, neurons

437   expressing low level GFPp65 or GFPp65ΔSE exhibited similar levels of normalized NF-

438   κB reporter activity, and stimulations were graphed relative to this level (set as 1.0,

439   Figure 3B). Ionomycin/PMA stimulation equivalently increased NF-κB reporter activity

440   in neurons expressing either GFPp65 or GFPp65ΔSE (1.86 ± 0.09 and 1.80 ± 0.09 fold,

441   p = 0.018 and p = 0.0002, respectively, compared to no stimulation). In contrast,

442   synaptic activation with low dose bicuculline increased NF-κB reporter expression by

443   2.58 ± 0.39 fold in neurons expressing GFPp65 while neurons expressing GFPp65ΔSE

444   showed no significant response (p = 0.0001 and p = 0.389, respectively, compared to

445   no stimulation (Figure 3B). Synaptic stimulation with glycine increased NF-κB reporter

446   expression by 2.52 ± 0.21 fold in neurons expressing GFPp65 while neurons expressing

447   GFPp65ΔSE showed no significant response (p = 0.0001 and p = 0.692, respectively,

448   compared to no stimulation (Figure 3B). Collectively, this data indicates that

449   GFPp65ΔSE, which lacks enrichment at dendritic spines, can support NF-κB-dependent

450   gene expression in response to a diffuse stimulus, but is ineffective in supporting NF-

451   κB-dependent gene expression in response to two stimuli originating in the synaptic

452   compartment. These findings are consistent with a role for the spine-enriched pool of

453   NF-κB in mediating NF-κB-dependent gene expression in response to excitatory

454   synaptic stimuli.

455

456   **Response to synaptic stimuli requires the canonical NF-κB pathway**

457   Previous work has shown that signaling components required for NF-κB

458   activation, including degradation of the inhibitor of NF-κB (IκB), are present at synapses

459   (Meffert et al., 2003). The failure of synaptic stimulation to induce NF-κB-dependent

460   transcription in neurons lacking spine-enriched NF-κB could be due to a necessity for

461   localization of the NF-κB/IκB complex in proximity to stimuli incoming at synapses. To

462   test whether synaptic and diffuse stimuli utilize distinct or shared NF-κB induction

463   pathways, we assessed the effect of inhibition of the canonical activation pathway

464   through IKK, using both small molecule (Skaug et al., 2011; Liu et al., 2012) and peptide

465   IKK inhibitors(May et al., 2000; Solt et al., 2007; Solt et al., 2009). The selective small

466   molecule IKK inhibitor, TPCA-1, or a cell-permeant nemo (IKKγ) binding domain IKK

467   inhibitor peptide (TAT-NBD) each prevented increased NF-κB activation by diffuse or by

468   synaptic stimuli (Figure 3C; Ionomycin/PMA, Bicuculline, or Glycine) in hippocampal

469   neurons, compared to control stimulations in vehicle alone (Ionomycin/PMA: 1.91 ±

470   0.24, p = 0.043, Bicuculline: 2.72 ± 0.31, p = 0.0001, glycine: 2.41 ± 0.25, p = 0.0007) or

471   control TAT peptide (Ionomycin/PMA: 2.01 ± 0.20, p = 0.014, Bicuculline: 2.72 ± 0.33, p

472   = 0.0001, glycine: 2.30 ± 0.21, p = 0.002).).   These data demonstrate that NF-κB

473   activation by diffuse and synaptic stimuli both proceed through the canonical IKK-

474   dependent pathway, consistent with a difference in localization of the NF-κB complex

475   near synapses underlying the loss of responsiveness in neurons which were lacking

476   spine-enriched NF-κB.

477

478   **Spine-enriched NF-κB in dendritic spine development**

479   During developmental periods of rapid spine and synapse formation, high basal

480   levels of excitatory glutamatergic synaptic transmission produce elevated NF-κB

481   transcriptional activity which is required for the *in vitro* and *in vivo* production of normal

482   hippocampal pyramidal dendritic spine density, spine maturity, and corresponding

483   synaptic currents (Boersma et al., 2011; Schmeisser et al., 2012). We harnessed this

484   assay to further probe function of the spine-enriched pool of NF-κB by testing its

485   requirement in a biologically relevant readout, dendritic spine formation, downstream of

486   synaptic stimulation. Hippocampal cultures deficient in endogenous p65 (from RelA$^{f/f}$

487   mice) were transfected with either GFP, wild-type p65 (GFPp65), or the p65 mutant

488   lacking spine-enrichment (GFPp65ΔSE) and pyramidal neurons assayed for dendritic

489   spine density and spine head volume by live confocal imaging during the period of rapid

490   spine formation (DIV 14 - 16) (Figure 4). Basal spine density in wild-type neurons

491   expressing GFP was 1.89 ± 0.23 spines / 10 μm, with an average spine head volume of

492   0.217 ± 0.028 μm^3. Loss of p65 (GFP + OHT) decreased spine density by 46.7 % (to

493   1.01 ± 0.08 spines / 10 μm) and average spine head volume by 40.4 % (to 0.129 ±

494   0.021 μm^3). Expression of GFPp65 in p65-deficient neurons rescued both spine density

495   (2.35 ± 0.27 spines / 10 μm) and spine head volume (0.258 ± 0.021 μm^3) to levels

496   indistinguishable from wild-type neurons. In contrast, dendritic spine density and

497   volumes in p65-deficient neurons expressing GFPp65ΔSE did not significantly differ

498   from neurons lacking p65 (GFP + OHT). Expression of GFPp65ΔSE in p65-deficient

499   neurons also failed to rescue spine density (1.53 ± 0.20 spines / 10 μm, p = 0.03) to

500   wild-type levels, and showed a corresponding trend toward failed rescue for spine head

501   volumes (0.154 ± 0.020 μm^3, p = 0.073). Endogenous p65 is required for the

502   development of normal spine size and density. The inability of GFPp65ΔSE to mimic

503   the effects of wild-type p65 on spine density and head volume indicates a critical

504   biological role for spatial localization of p65 to dendritic spines in supporting spine

505   growth, which relies upon NF-κB-dependent transcription (Boersma et al., 2011).

506

507   **DISCUSSION**

508   Healthy neural plasticity in the adult brain is enabled by the selective regulation

509   of gene expression following neuronal activity. Features that enable transcription

510   factors to differentiate neuronal stimuli, and to produce appropriate gene regulatory

511   responses are incompletely understood. In this work, we show that the enrichment of a

512   transcription factor in a discrete subcellular location, the dendritic spine head,

513   selectively facilitates responses to excitatory activity incoming through synapses, while

514   not being required for the response to more diffuse neuronal stimulation that does not

515   originate at synapses.

516   NF-κB is a pleiotropic transcription factor that functions broadly in the control of

517   genes promoting cellular and synapse growth, and for which evolutionarily conserved

518   requirements have been established in multiple assays of plasticity, learning, and

519   memory from crabs to fruit flies to mammals (Shrum and Meffert, 2008; Salles et al.,

520   2014). The characterization of NF-κB enrichment in dendritic spines presents an

521   interesting distinguishing feature, as relatively few transcription factors are known to

522   localize to discrete extranuclear regions. Other notable exceptions include CREB

523   (which has been reported in axons), and Stat3 and the transcription activator ELK-1

524   which have been reported in neuronal dendrites (Suzuki et al., 1998). We identify a 101

525   amino acid region of the p65 NF-κB subunit that is required for NF-κB enrichment in

526   dendritic spine heads. Overlapping mutants (Figure 2) suggest that the region of

527   importance for dendritic spine localization may be further narrowed to a 30 amino acid

528   sequence. No protein-protein or protein-RNA interaction motifs have been previously

529   characterized in this region of p65, which bears little conservation among other NF-κB

530   subunits. A motif scan (Scansite 4.0, MIT) does identify a Src homology 3 (SH3)

531   domain poly-proline binding motif in p65 which is conserved across mammals

532   (beginning at human P322, PRPPP), and is lacking in GFPp65ΔSE but present in all

533   spine-enriched constructs of p65 (Figure 2A,B). Binding of SH3 domains has been

534   implicated in mediating protein-protein interactions and clustering at synapses; for

535   example, MAGUK scaffolding proteins contain SH3 domains and are concentrated in

536   the postsynaptic densities of neuronal synapses (Sheng, 1996; McGee and Bredt,

537   1999). In previous work (Boersma et al., 2011), we demonstrated that a MAGUK, PSD-

538   95, is an NF-κB transcriptional target that is critical for NF-κB-mediated increases in

539   dendritic spine density. Additional analysis of the amino acid region implicated in spine-

540   enrichment of p65 by charge density showed that it contained the entirety of a long

541   stretch of uncharged amino acids (82 amino acids). When subjected to analysis for

542   protein disorder prediction (DISOPRED3, PSIPRED protein sequence analysis UCL;

543   (Jones and Cozzetto, 2015)) the p65 profile showed that the section implicated in spine

544   enrichment (amino acids, 305 – 406), was predicted with high confidence to contain an

545   intrinsically disordered region (IDR, lacking defined and ordered 3D structure). This is

546   particularly intriguing given the recently heightened interest in potential biological roles

547   of protein IDRs (Lin et al., 2015; Shin and Brangwynne, 2017; Wei et al., 2017).

548   Biochemical and ionic fluxes between the cytoplasm of spines and neighboring

549   dendritic shafts can be limited in mature spines, many of which have relatively thin

550   necks connected to the parent dendrite (Bourne and Harris, 2008; Adrian et al., 2014).

551   This type of compartmentalization may confer particular value to spine-enrichment of

552   NF-κB in sensing synaptic excitation and mediating activity-responsive gene expression

553   in neurons. Previous work has shown that neuronal NF-κB can be activated by sub-

554   membranous calcium elevation signaling through calcium-calmodulin protein kinase II

555   (CaMKIIα, a kinase highly abundant in the post-synaptic density), in hippocampal

556   neurons as well as in isolated synapses (Meffert et al., 2003). In this report, we

557   demonstrate a role for local enrichment in dendritic spines in shaping the stimulus

558   specificity of NF-κB. The p65 mutant engineered to lack spine head enrichment,

559   p65ΔSE, retains inherent NF-κB transcriptional activity and transcriptional response to

560   diffuse stimulation, but exhibits deficiency in mediating NF-κB-dependent transcription

561   to modest stimulation incoming through excitatory synapses and fails to support normal

562   head volume and density of dendritic spines. The enrichment of NF-κB in dendritic

563   spine heads raises the possibility of a potential contribution of local protein-protein

564   interactions not requiring transcription to these phenotypes. However, using

565   transcriptionally-inactive mutants of p65 (including p65ΔTAD), we previously found that

566   activity-dependent enhancement of dendritic spine size and density required cell-

567   autonomous NF-κB-dependent transcription (Boersma et al., 2011).

568   NF-κB activation by either diffuse or synaptic stimulation required the canonical

569   IKK-mediated pathway, previously shown to participate in synaptic plasticity (Russo et

570   al., 2009). This shared feature further supports the importance of subcellular

571   localization of the initiating stimulus in defining the requirement for spine-enriched NF-

572   κB. It is possible that enrichment at the sites of incoming excitatory stimuli might also

573   regulate additional features of gene expression, by impacting the kinetics, magnitude, or

574   duration of NF-κB induction following stimulation. Since the exact sequence of the NF-

575   κB DNA-response elements in a promoter/enhancer region is reported to code a

576 preference for binding to (and activation by) particular NF-κB dimers under some

577 conditions (Wang et al., 2012), selective activation of p65-containing NF-κB dimers that

578 are spine-enriched might have the potential to impact the specificity of NF-κB-

579 dependent gene expression. Collectively, this work highlights spine head enrichment as

580 a feature contributing to activity-responsive gene expression by NF-κB, a transcription

581 factor implicated in multiple contexts of experience-dependent plasticity.

582

583 **AUTHOR CONTRIBUTIONS**

584 E.C.D., M.C.H.B, and M.K.M. conceived and designed the experiments. E.C.D.,

585 M.C.H.B, and M.K.M performed all experiments and data analyses in the laboratory of

586 M.K.M. M.K.M. and E.C.D wrote the manuscript. This work was funded by grants to

587 M.K.M. M.K.M initiated and supervised the project.

588
589
590 **REFERENCES**
591

592 Adrian M, Kusters R, Wierenga CJ, Storm C, Hoogenraad CC, Kapitein LC (2014)
593 Barriers in the brain: resolving dendritic spine morphology and compartmentalization.
594 Front Neuroanat 8:142.

595 Andersen P, Sundberg SH, Sveen O, Swann JW, Wigstrom H (1980) Possible
596 mechanisms for long-lasting potentiation of synaptic transmission in hippocampal slices
597 from guinea-pigs. The Journal of physiology 302:463-482.

598 Araki Y, Zeng M, Zhang M, Huganir Richard L (2015) Rapid Dispersion of SynGAP from
599 Synaptic Spines Triggers AMPA Receptor Insertion and Spine Enlargement during LTP.
600 Neuron 85:173-189.

601 Baichwal VR, Baeuerle PA (1997) Activate NF-kappa B or die? Current biology : CB
602 7:R94-96.

603 Boersma MC, Dresselhaus EC, De Biase LM, Mihalas AB, Bergles DE, Meffert MK
604 (2011) A requirement for nuclear factor-kappaB in developmental and plasticity-

605   associated synaptogenesis. The Journal of neuroscience : the official journal of the
606   Society for Neuroscience 31:5414-5425.

607   Bourne JN, Harris KM (2008) Balancing structure and function at hippocampal dendritic
608   spines. Annu Rev Neurosci 31:47-67.

609   De Lorenzi R, Gareus R, Fengler S, Pasparakis M (2009) GFP-p65 knock-in mice as a
610   tool to study NF-kappaB dynamics in vivo. Genesis 47:323-329.

611   Fortin DA, Davare MA, Srivastava T, Brady JD, Nygaard S, Derkach VA, Soderling TR
612   (2010) Long-Term Potentiation-Dependent Spine Enlargement Requires Synaptic Ca^{2+}-
613   Permeable AMPA Receptors Recruited by CaM-Kinase I. The Journal of neuroscience :
614   the official journal of the Society for Neuroscience 30:11565-11575.

615   Freudenthal R, Romano A (2000) Participation of Rel/NF-kappaB transcription factors in
616   long-term memory in the crab Chasmagnathus. Brain research 855:274-281.

617   Freudenthal R, Boccia MM, Acosta GB, Blake MG, Merlo E, Baratti CM, Romano A
618   (2005) NF-kappaB transcription factor is required for inhibitory avoidance long-term
619   memory in mice. The European journal of neuroscience 21:2845-2852.

620   Harris KM, Jensen FE, Tsao B (1992) Three-dimensional structure of dendritic spines
621   and synapses in rat hippocampus (CA1) at postnatal day 15 and adult ages:
622   implications for the maturation of synaptic physiology and long-term potentiation. The
623   Journal of neuroscience : the official journal of the Society for Neuroscience 12:2685-
624   2705.

625   Heckscher ES, Fetter RD, Marek KW, Albin SD, Davis GW (2007) NF-kappaB, IkappaB,
626   and IRAK control glutamate receptor density at the Drosophila NMJ. Neuron 55:859-
627   873.

628   Hering H, Sheng M (2001) Dendritic spines: structure, dynamics and regulation. Nature
629   reviews Neuroscience 2:880-888.

630   Holtmaat A, Svoboda K (2009) Experience-dependent structural synaptic plasticity in
631   the mammalian brain. Nature reviews Neuroscience 10:647-658.

632   Jones DT, Cozzetto D (2015) DISOPRED3: precise disordered region predictions with
633   annotated protein-binding activity. Bioinformatics 31:857-863.

634   Kaltschmidt B, Ndiaye D, Korte M, Pothion S, Arbibe L, Prullage M, Pfeiffer J, Lindecke
635   A, Staiger V, Israel A, Kaltschmidt C, Memet S (2006) NF-kappaB regulates spatial
636   memory formation and synaptic plasticity through protein kinase A/CREB signaling. Mol
637   Cell Biol 26:2936-2946.

638   Kaltschmidt C, Kaltschmidt B, Baeuerle PA (1993) Brain synapses contain inducible
639   forms of the transcription factor NF-kappa B. Mechanisms of development 43:135-147.

640　Lin Y, Protter DSW, Rosen MK, Parker R (2015) Formation and Maturation of Phase
641　Separated Liquid Droplets by RNA Binding Proteins. Molecular cell 60:208-219.

642　Liu F, Xia Y, Parker AS, Verma IM (2012) IKK biology. Immunological Reviews 246:239-
643　253.

644　May MJ, D'Acquisto F, Madge LA, Glöckner J, Pober JS, Ghosh S (2000) Selective
645　Inhibition of NF-κB Activation by a Peptide That Blocks the Interaction of NEMO with the
646　IκB Kinase Complex. Science 289:1550-1554.

647　McGee AW, Bredt DS (1999) Identification of an intramolecular interaction between the
648　SH3 and guanylate kinase domains of PSD-95. The Journal of biological chemistry
649　274:17431-17436.

650　Meffert MK, Chang JM, Wiltgen BJ, Fanselow MS, Baltimore D (2003) NF-kappa B
651　functions in synaptic signaling and behavior. Nature neuroscience 6:1072-1078.

652　Mihalas AB, Araki Y, Huganir RL, Meffert MK (2013) Opposing action of nuclear factor
653　kappaB and Polo-like kinases determines a homeostatic end point for excitatory
654　synaptic adaptation. The Journal of neuroscience : the official journal of the Society for
655　Neuroscience 33:16490-16501.

656　Nimchinsky EA, Sabatini BL, Svoboda K (2002) Structure and function of dendritic
657　spines. Annual review of physiology 64:313-353.

658　Noguchi J, Matsuzaki M, Ellis-Davies GC, Kasai H (2005) Spine-neck geometry
659　determines NMDA receptor-dependent Ca2+ signaling in dendrites. Neuron 46:609-622.

660　Nonaka M, Kim R, Sharry S, Matsushima A, Takemoto-Kimura S, Bito H (2014)
661　Towards a better understanding of cognitive behaviors regulated by gene expression
662　downstream of activity-dependent transcription factors. Neurobiology of learning and
663　memory 115:21-29.

664　O'Riordan KJ, Huang IC, Pizzi M, Spano P, Boroni F, Egli R, Desai P, Fitch O, Malone
665　L, Ahn HJ, Liou HC, Sweatt JD, Levenson JM (2006) Regulation of nuclear factor
666　kappaB in the hippocampus by group I metabotropic glutamate receptors. The Journal
667　of neuroscience : the official journal of the Society for Neuroscience 26:4870-4879.

668　Peters A, Kaiserman-Abramof IR (1970) The small pyramidal neuron of the rat cerebral
669　cortex. The perikaryon, dendrites and spines. The American journal of anatomy
670　127:321-355.

671　Russo SJ et al. (2009) NFκB Signaling Regulates Neuronal Morphology and Cocaine
672　Reward. The Journal of neuroscience : the official journal of the Society for
673　Neuroscience 29:3529-3537.

674　Salles A, Romano A, Freudenthal R (2014) Synaptic NF-kappa B pathway in neuronal
675　plasticity and memory. Journal of physiology, Paris 108:256-262.

676 Schmeisser MJ, Baumann B, Johannsen S, Vindedal GF, Jensen V, Hvalby OC,
677 Sprengel R, Seither J, Maqbool A, Magnutzki A, Lattke M, Oswald F, Boeckers TM,
678 Wirth T (2012) IkappaB kinase/nuclear factor kappaB-dependent insulin-like growth
679 factor 2 (Igf2) expression regulates synapse formation and spine maturation via Igf2
680 receptor signaling. The Journal of neuroscience : the official journal of the Society for
681 Neuroscience 32:5688-5703.

682 Sheng M (1996) PDZs and receptor/channel clustering: rounding up the latest suspects.
683 Neuron 17:575-578.

684 Shin Y, Brangwynne CP (2017) Liquid phase condensation in cell physiology and
685 disease. Science 357.

686 Shrum CK, Meffert MK (2008) The NF-kB family in learning and memory. In: Learning
687 And Memory: A Comprehensive Reference (Byrne J, ed), pp *567 - 586*. Oxford: Elsevier
688 Ltd.

689 Skaug B, Chen J, Du F, He J, Ma A, Chen ZJ (2011) Direct, Non-catalytic Mechanism of
690 IKK Inhibition by A20. Molecular Cell 44:559-571.

691 Solt LA, Madge LA, May MJ (2009) NEMO-binding Domains of Both IKKα and IKKβ
692 Regulate IκB Kinase Complex Assembly and Classical NF-κB Activation. The Journal of
693 biological chemistry 284:27596-27608.

694 Solt LA, Madge LA, Orange JS, May MJ (2007) Interleukin-1-induced NF-κB Activation
695 Is NEMO-dependent but Does Not Require IKKβ. The Journal of biological chemistry
696 282:8724-8733.

697 Suzuki T, Usuda N, Ishiguro H, Mitake S, Nagatsu T, Okumura-Noji K (1998)
698 Occurrence of a transcription factor, cAMP response element-binding protein (CREB),
699 in the postsynaptic sites of the brain. Brain research Molecular brain research 61:69-77.

700 Tada T, Sheng M (2006) Molecular mechanisms of dendritic spine morphogenesis.
701 Current opinion in neurobiology 16:95-101.

702 Wang VY, Huang W, Asagiri M, Spann N, Hoffmann A, Glass C, Ghosh G (2012) The
703 transcriptional specificity of NF-kappaB dimers is coded within the kappaB DNA
704 response elements. Cell Rep 2:824-839.

705 Wei M-T, Elbaum-Garfinkle S, Holehouse AS, Chen CC-H, Feric M, Arnold CB,
706 Priestley RD, Pappu RV, Brangwynne CP (2017) Phase behaviour of disordered
707 proteins underlying low density and high permeability of liquid organelles. Nat Chem
708 9:1118.

709 Yuste R, Majewska A, Holthoff K (2000) From form to function: calcium
710 compartmentalization in dendritic spines. Nature neuroscience 3:653-659.

711

712

Figure Legends:

Figure 1: *p65 is sufficient for NF-κB enrichment in dendritic spines of hippocampal pyramidal neurons.* A) EMSA from synapses isolated from wild-type ($p50^{+/+}$) or p50-deficient ($p50^{-/-}$) murine hippocampi. NF-κB was detected using a radiolabelled oligonucleotide κB probe and specific subunits identified by antibody-supershifted bands. DOC was used to allow detection of occult (inactive) NF-κB. p65:p65 homodimers detected in $p50^{-/-}$ isolated synapses from all (4) biological replicates of the experiment. B) Confocal images of live DIV17 hippocampal neurons co-expressing mCherry with either GFP, GFPp65 or GFPp50, as indicated. Graph shows % enrichment of GFPp65 or GFPp50, relative to GFP, as described in Materials and Methods. Scale bar = 5 μm. Error bars show SEM. *p = 3.8 x 10^{-10}. C) Diagram representing spine measurements; dashed lines indicate diameter. D) Analysis of spine maturity from dendrites expressing GFPp65. Percent enrichment of GFPp65 in dendritic spines is calculated and binned according to spine size. Spine size was determined by a ratio of the spine head diameter to the spine neck diameter. Scale bar = 1 μm. Error bars show SEM. *p-values as compared to enrichment for spines <1 are as follows: for 1-3 p = 0.004, for 3-4 p = 0.002, for >4 p = 0.003. E) Confocal images of hippocampal pyramidal neurons co-expressing GFP and mCherry (left) or expressing mCherry fluorescent protein and GFPp65 from the endogenous RelA locus (right) and immunostained for GFP and mCherry. Graph shows percent enrichment of GFP and endogenously expressed GFPp65. Scale bar = 5 μm. Error bars show SEM. *p = 1.4x10^{-5}.

735

736 **Figure 2**: *Identification of non-spine enriched mutants of p65.* A) Diagram of p65 and

737 p65 deletion and truncation constructs. B) Graph showing % enrichment of GFP-

738 tagged p65 and GFP-tagged p65 deletion and truncation constructs. Enrichment is

739 determined as described in Materials and Methods. Error bars show SEM. *p-values as

740 compared to GFP condition are as follows: for GFPp65 $p = 2.5 \times 10^{-30}$, for GFPp65Δ1-

741 298 $p = 4.7 \times 10^{-15}$, for GFPp65Δ335-442 $p = 9.5 \times 10^{-8}$, and # data from GFPp65ΔTAD

742 condition was previously presented (Boersma et al., 2011) in a different format. C)

743 Representative confocal images from live murine hippocampal neurons co-expressing

744 mCherry with GFP-tagged p65 deletion or truncation constructs or wild-type p65. Scale

745 bar = 5 μm. D) p65 constructs were expressed in 293T cells at equivalent levels and

746 migrate at their expected molecular weights by immunoblot of lysates. Expected

747 molecular weights (kDa) as follows: GFPp65: 87, GFPp65ΔTAD: 76, GFPp65Δ1-298:

748 53, GFPp65Δ1002-1326: 76, GFPp65Δ916-1218: 76, GFPp65Δ305-551: 62, GFP: 27.

749 E) Expression of p65 constructs does not significantly alter measures of neuronal

750 health. Percent of neurons scoring positive in confocal imaging for cytoplasmic

751 blebbing/beading or for pyknotic nuclear morphology using Hoechst staining from

752 hippocampal neurons co-expressing mCherry with either GFP, GFPp65, or

753 GFPp65ΔSE. Staurosporine treatment of GFP-expressing neurons serves as a positive

754 control; experimenter was blinded to condition during all imaging and analysis. Cells

755 were scored as positive or negative (see Materials and Methods) and percent positive

756 plotted per condition (precluding SEM calculation).

757

758 **Figure 3**: *A p65 mutant lacking spine-enrichment is selectively deficient in response to*

759 *synaptic stimulation.* A) Inherent transactivation potential of wild-type p65 and p65

760 lacking spine-enrichment (p65ΔSE) are not distinguishable. Reporter assay for dose-

761 titrated expression of GFPp65 or GFPp65ΔSE in HEK293T cells co-expressing NF-κB

762 luciferase reporter and constitutive β-galactosidase used for normalization (Left). Fold

763 induction calculated as described in Materials and Methods. Representative

764 immunoblot of dose titration (Right). B) NF-κB luciferase assay of p65-deficient

765 neurons expressing full length GFPp65 or GFPp65ΔSE and either mock-stimulated or

766 stimulated with bicuculline (30 μM for 30 seconds), with ionomycin/PMA (3.5 hr), or with

767 glycine (100 μM for 10 min). *$p = 0.018$ compared to GFPp65 no stimulation. **$p =$

768 0.0002 compared to GFPp65ΔSE no stimulation. ****$p = 0.0001$ compared to GFPp65

769 no stimulation. For neurons expressing GFPp65ΔSE, NF-κB reporter activity in

770 response to bicuculline or glycine does not differ significantly from the no stimulation

771 condition. Representative immunoblot (inset) illustrating similar levels of expressed

772 protein for GFPp65 or GFPp65ΔSE in these experiments. C) NF-κB luciferase assay of

773 wild-type neurons either mock-stimulated or stimulated with ionomycin/PMA (2 μM and

774 50 ng/ml), bicuculline (30 μM for 30 seconds), or with glycine (150 μM for 10 min) and

775 treated with either TPCA1 (4 μM) or TAT-NBD (20 μM) or their respective vehicle or

776 TAT controls. *$p = 0.04$, ***$p = 0.0007$, ****$p = 0.0001$, all compared to no stimulation

777 which was set to 1. Error bars indicate SEM.
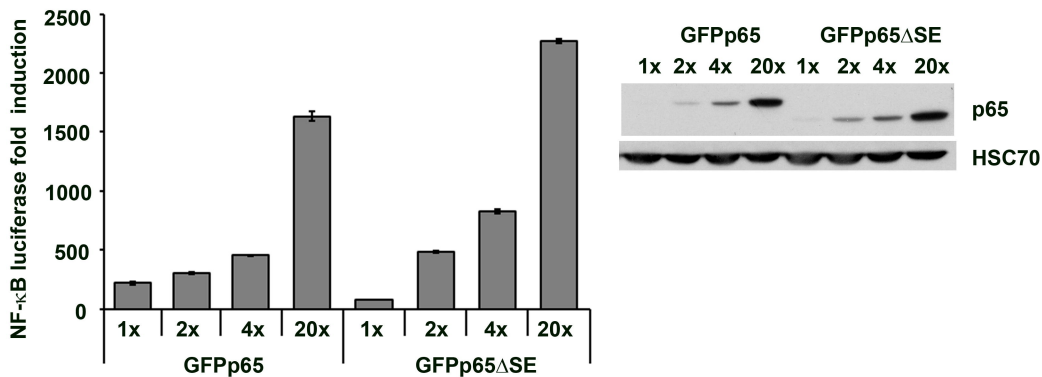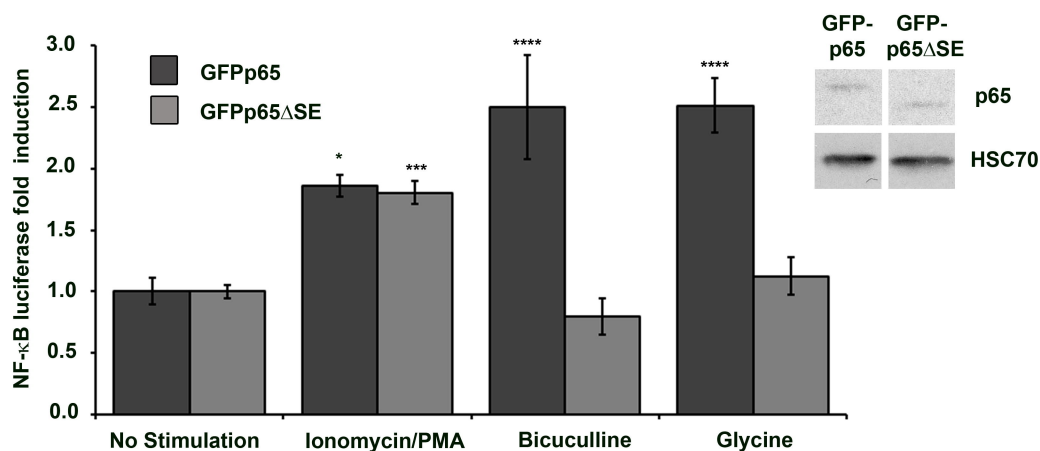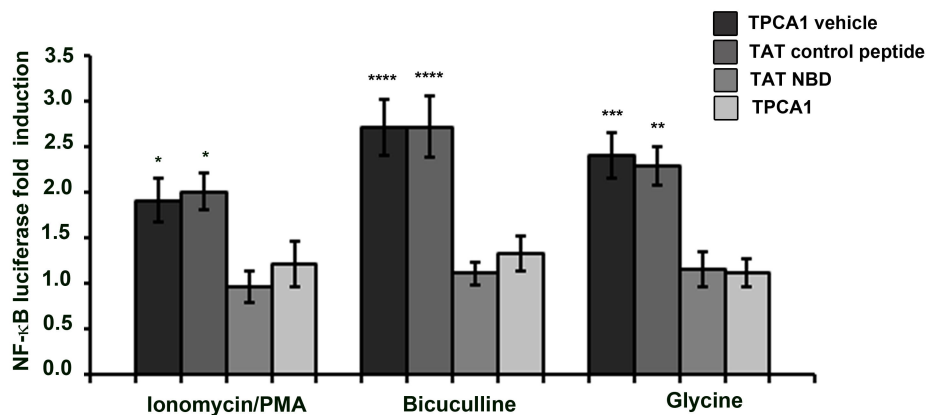
778

779 **Figure 4:** *p65 lacking spine-enrichment fails to rescue neuronal dendritic spine density*

780 *and size during spinogenesis.* Loss of endogenous p65 (OHT) in pyramidal neurons
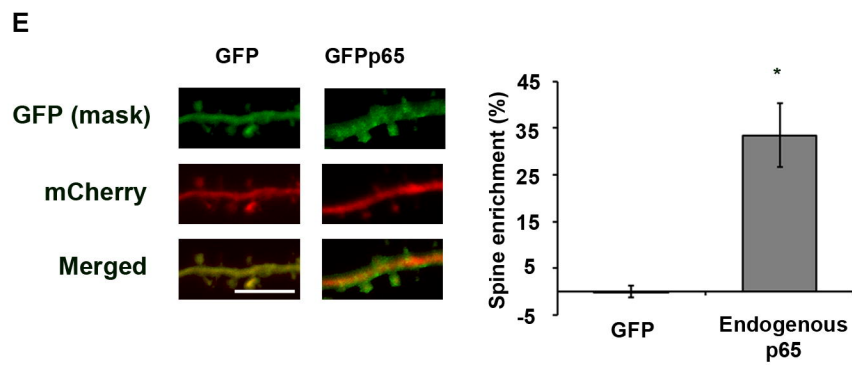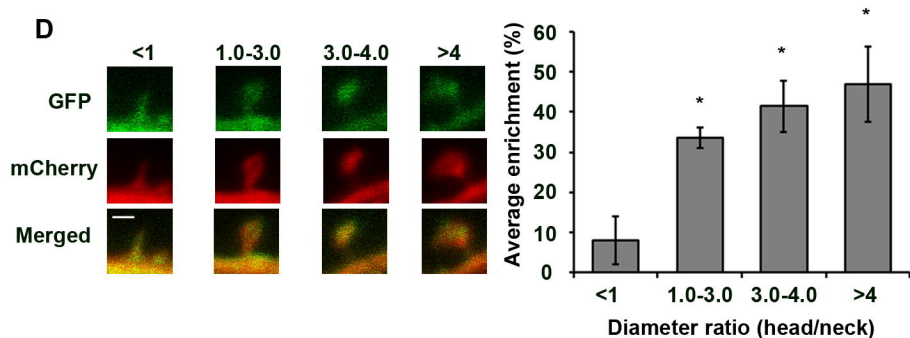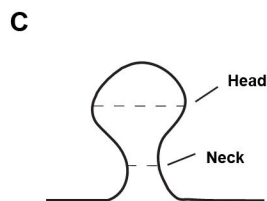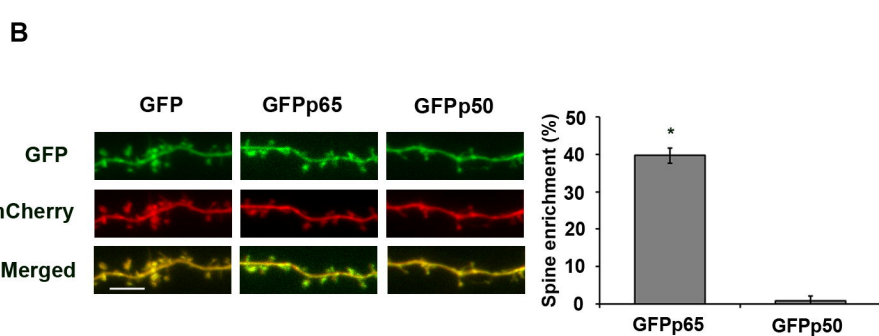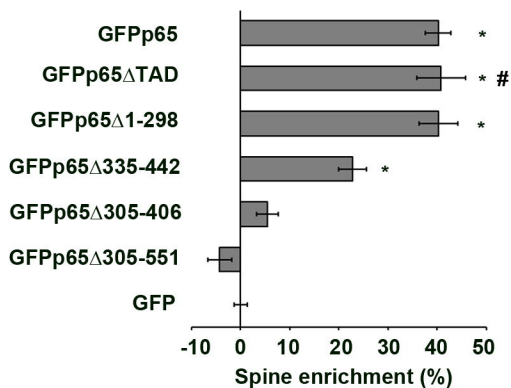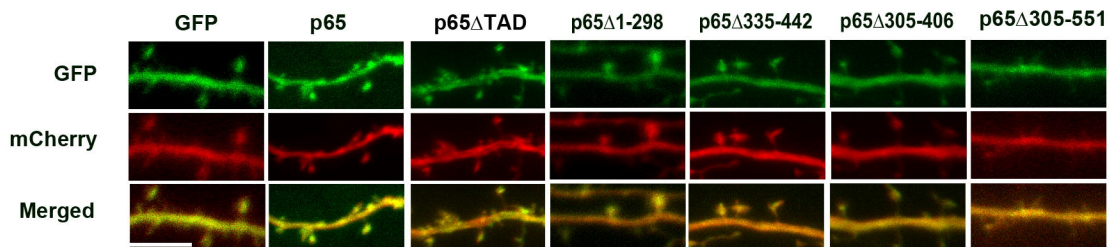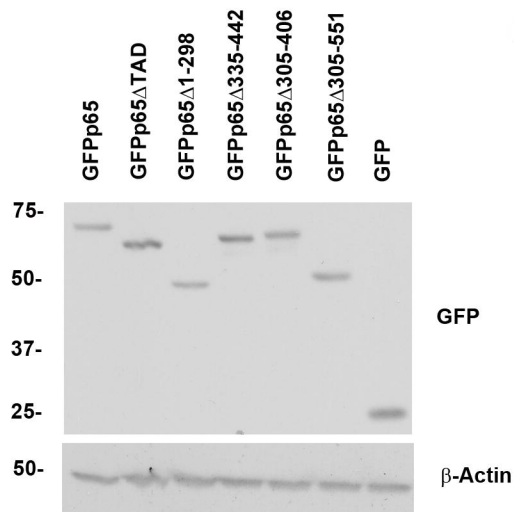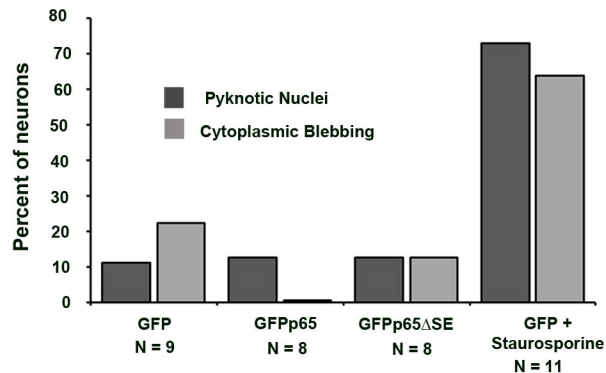
781   (DIV 15-16) significantly decreases dendritic spine density (GFP + OHT, *p = .0047,

782   panel A) and spine head volume (GFP + OHT, *p = 0.0151, panel C), compared to

783   GFP. A) Expression of wild-type p65 (GFPp65, p = 0.212), but not p65 lacking spine

784   enrichment (GFPp65ΔSE, *p = 0.024), rescues dendritic spine density back to baseline

785   (GFP) levels in hippocampal pyramidal neurons conditionally deficient in p65 (OHT)

786   (ANOVA, p = 0.0009).   B) Representative confocal projections (with co-expressed

787   mCherry) of dendrites from live murine hippocampal neurons used to calculate spine

788   densities (A). Scale bar = 5 µm. C) Expression of wild-type p65 (GFPp65, p = 0.262)

789   rescues spine head volume back to baseline (GFP) levels in p65-deficient hippocampal

790   pyramidal neurons. Expression of GFPp65ΔSE shows a trend towards failed rescue of

791   spine head volume (p = 0.073, compared to GFP) (ANOVA, p = 0.0056) and spine head

792   volumes which are significantly different from GFPp65-expressing neurons (#, p =

793   0.0006, compared to GFPp65 + OHT). D) Representative confocal projections (with co-

794   expressed mCherry) from live murine hippocampal neurons used to calculate spine

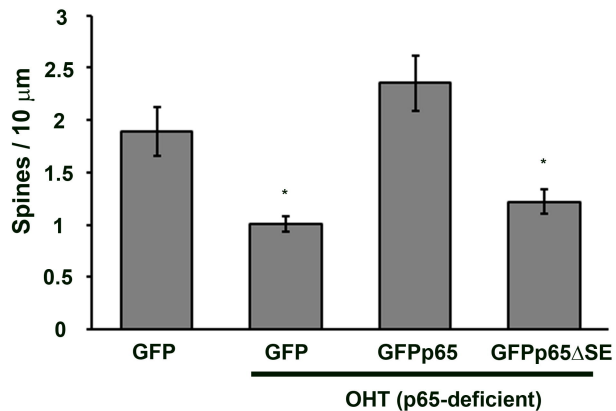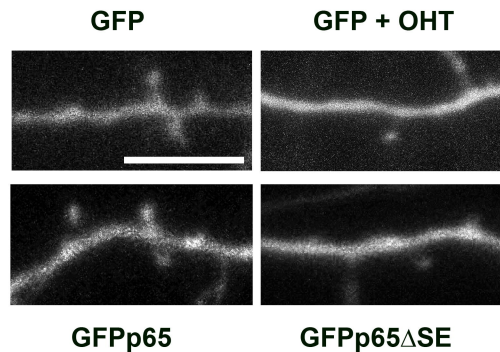795   head volumes (C). Scale bar = 1.0 µm. Error bars indicate SEM.

796

797

A — 3T3, p50 +/+ (syn. + DOC, mut.κB; syn.; syn. + DOC), p50 -/- (syn. + DOC, mut.κB; syn.; syn. + DOC; syn. + DOC + p52 Ab; syn. + DOC + c-Rel Ab; syn. + DOC + RelB Ab; syn. + DOC + p65 Ab)

p65:p65, p65:p50, Supershifted Band

B — GFP, GFPp65, GFPp50; GFP, mCherry, Merged; Spine enrichment (%): GFPp65, GFPp50

C — Head, Neck

D — <1, 1.0-3.0, 3.0-4.0, >4; GFP, mCherry, Merged; Average enrichment (%) vs Diameter ratio (head/neck): <1, 1.0-3.0, 3.0-4.0, >4

E — GFP, GFPp65; GFP (mask), mCherry, Merged; Spine enrichment (%): GFP, Endogenous p65

A

Spines / 10 μm

- GFP
- GFP
- GFPp65
- GFPp65ΔSE

OHT (p65-deficient)

B

| GFP | GFP + OHT |
| GFPp65 | GFPp65ΔSE |

C

Spine head volume (μm³)

- GFP
- GFP
- GFPp65
- GFPp65ΔSE

OHT (p65-deficient)

D

| GFP | GFP + OHT |
| GFPp65 | GFP p65ΔSE |